

Stroke Tissue Outcome Prediction Using A Spatially-Correlated Model

Viet Ha Nguyen^(1,3), Gene Cooperman⁽³⁾, Nina Menenzes⁽²⁾, Chloe J. Lopez⁽²⁾,
Christopher Melinosky⁽²⁾, Ona Wu⁽²⁾, Hakan Ay⁽⁴⁾, Yawu Liu⁽⁵⁾, Juho Nuutinen⁽⁵⁾,
Hannu J. Aronen⁽⁵⁾, Jari Karonen⁽⁵⁾, A. Gregory Sorensen⁽²⁾, Walter J. Koroshetz^(4,6),
Homer H. Pien⁽²⁾

⁽¹⁾A.N.Lab Inc, Hanoi, Vietnam

⁽²⁾ Department of Radiology, Massachusetts General Hospital, Boston, MA 02129

⁽³⁾ College of Computer and Information Science, Northeastern University, Boston, MA 02115

⁽⁴⁾ Department of Neurology, Massachusetts General Hospital, Boston, MA 02129

⁽⁵⁾ Helsinki University Central Hospital, Helsinki, Finland

⁽⁶⁾ National Institutes of Health / NINDS, Bethesda, MD 20892

In acute ischemic stroke the early and accurate prediction of tissue outcome is important to decisions regarding therapy. One proposed prediction approach is to combine structural, perfusion, and diffusion MRI in a generalized linear model (GLM) to predict voxel outcome. Such a model, however, does not account for the spatial correlation likely to be present in voxels that result in infarction. A simple spatial correlation model extension of GLM is presented in this paper; showing moderate improvement in the prediction accuracy.

1. Introduction

Stroke is a leading health problem in the United States. With approximately 600,000 new or recurrent cases of stroke each year, it is the third leading cause of death and the principal cause of long-term disability (1). Strokes can be ischemic or hemorrhagic; approximately 85% of all strokes are ischemic (1). Clinically, it is important to render an accurate prediction of the location and extent of the stroke as early after onset of stroke symptoms as possible, since such prognoses impact the therapeutic regimen (2). The purpose of this paper is to discuss the development of a new technique which appears to increase the accuracy with which ischemic stroke tissue outcome, on a voxel-by-voxel basis, can be predicted.

Stroke imaging is conventionally performed with either computed tomography (CT) or magnetic resonance (MR) imaging. MR in particular offers both soft tissue contrast and functional imaging capability (3). By measuring the reduction in the amount of free molecular movement of water molecules as cells undergo cytotoxic edema, MR diffusion has been shown to be a sensitive indicator of stroke (4-6). Similarly, MR perfusion imaging utilizes a contrast agent to permit the visualization and computation of the rate with which the contrast agent flows into a region, and such perfusion measurements have also been shown to offer insights into the progression of ischemic stroke (7,8). In this paper we focus on MR imaging

using a combination of anatomical, perfusion, diffusion imaging.

Several techniques have been explored for combining different types of MR data, including ISODATA clustering, thresholding, and generalized linear model (GLM) (9-11). GLM provides a mapping from the feature space to an outcome-probability space, where the probabilities indicate the likelihood of each voxel becoming infarcted. However, the GLM (and other models that have been examined), assumes independence among the feature vectors – an assumption that can likely be improved since the final infarcted regions are generally contiguous regions instead of isolated voxels. Physiologically, it seems plausible that if a voxel is to become infarcted due to lack of oxygenation, then its neighboring voxel is also likely to suffer the same fate. As such, we sought to identify and implement an alternative linear model in which spatial correlations can be readily modeled. To that end, we've implemented a spatial autoregressive model (SAR) from the field of economics; SAR models appear to both provide the desired qualities and produce improved results over GLM (13,14). Although alternative models (e.g., Markov random field) can be used to incorporate spatial correlations, SAR is attractive because it is a generalization of GLM, making it feasible to assess the incremental value of spatial correlation.

2. Theory

Wu et al (12) developed a supervised-learning model (generalized linear model, or GLM) which outputs a

* Suite 9.9, 9F, A4 Building, ThangLong International Village, Tran Dang Ninh, Cau Giay, Hanoi, Vietnam.
E-mail: vietha@anlab.jp

continuous value (ranging from 0 to 1) representing the risk of future infarction for each tissue voxel. The prediction is performed on six channels of MR images scanned within 12 hours of symptom onset. The six channels are: (i) T2-weighted anatomical images; (ii) diffusion-weighted images (DWI); (iii) apparent diffusion coefficient of water (ADC); (iv) relative cerebral blood volume (CBV); (v) relative cerebral blood flow (CBF), and (vi) mean transit time (MTT).

The probability of tissue infarction for voxel i can be represented by the logistic function

$$P_i = \frac{1}{1 + e^{-Y_i}}$$

where Y_i is a linear function of different MR channel values at voxel i :

$$Y_i = \alpha + \beta_1 \cdot T2_i + \beta_2 \cdot DWI_i + \beta_3 \cdot ADC_i + \beta_4 \cdot CBV_i + \beta_5 \cdot CBF_i + \beta_6 \cdot MTT_i + \varepsilon_i$$

The coefficients $\alpha, \beta_1, \dots, \beta_6$ are variables to be estimated, and ε_i denotes the error term. Let n denote the total number of voxels, k the number of parameters (here $k = 6$), this equation can be represented by $Y = \alpha + X\beta + \varepsilon$, where X is a $n \times k$ matrix containing the input values of the k MR channels for each of n voxels; Y is a vector of size n , β is a vector of k coefficients, α is a constant representing the bias or intercept term, and ε denotes a vector of size n representing the random effect of the observations. The error terms ε are typically assumed to have a normal distribution with a mean of 0.

A supervised approach, logistic regression, is used to estimate β and α . Training is performed by utilizing each subject's follow-up MR studies, in which the regions of final infarction have fully stabilized. Using these follow-up studies, a neuroradiologist first identifies regions of infarction; a binary image denoting the infarcted region is created and used as the target classification during supervised learning.

Spatial Autoregression Model (SAR)

In contrast to GLM where every voxel is treated independently, a simple spatial correlation model was used to assess the importance of such correlation models. More specifically, the SAR model extends the GLM by incorporating a recursive correlation term: $Y = \alpha + X\beta + \rho WY + \varepsilon$, where W is a $n \times n$ matrix representing the correlational structure, ρ is a coefficient representing the magnitude of the correlational effect (14). The W matrix is user defined where W_{ij} is equal to 1 if i, j are neighbors, and 0 otherwise, while the coefficient ρ is estimated algorithmically. By convention, the W matrix is normalized such that the sum of each row equals 1.

The term ρWY represents the spatial correlation. It can be seen that WY is a vector of size n , and the i^{th} element of WY is the sum of the outcome values of the neighbors of the voxel i . The coefficient ρ expresses the extent to which the sum of the neighboring outcomes contributes to the outcome at the target voxel.

Note that SAR is a recursive model. The vector of outcome Y in the term ρWY on the right-hand side is identical to the vector of outcome Y on the left-hand side of the model's equation. As a result, SAR is able to model a spatial correlation that propagates over many voxels, while using a simple adjacency matrix W that specifies only immediate neighbors.

3. Methods

Data analysis was performed retrospectively using MR images acquired from 74 patients. Patient demographics and stroke etiology are summarized in Table I. The data used consist of, for each patient (see Figure 1): (i) six channels of MR data acquired within 12 hours of symptom onset; the six channels are: T2, ADC, DWI, CBV, CBF, MTT; (ii) diffusion lesion (DWI lesion) and perfusion lesion (PWI lesion) determined from the above 6 MR channels by neuroradiologists blinded to the predictive results; (iii) a binary map of actual outcome determined from follow-up MRI by neuroradiologists blinded to the predictive results. A voxel is marked as 1 if it is infarcted on the follow-up exam, and 0 otherwise.

Prior to invoking the GLM model, the data is pre-processed through normalization, re-sampling, and extraction of training regions. For normalization, each channel of data is normalized by dividing by the average value of that MR channel over the normal region. The normal region is chosen to be the mirror mapping of the PWI lesion on the contralateral hemisphere of the same patient. All images in the dataset were re-sampled using bicubic splines to a consistent in-plane resolution of 1.56×1.56 mm. Lastly, the union of the PWI/DWI lesions is chosen as the training and testing regions.

4. Results

Both GLM and SAR models were evaluated on the 74-patient dataset described previously. A jackknifing approach – where the test result for each patient was obtained by using data from all other patients as training data – was used. To evaluate the prediction accuracy of each algorithm, we used two standard metrics: the area under the ROC (receiver operating characteristic) curve (AUC), and the maximum correct classification rate. The ROC curve for each subject is generated by plotting the true-positive ratio (sensitivity) against the false-positive ratio (1-specificity). The AUC is

calculated for each subject using numerical integration. The correct classification rate is defined as the sum of the true positive rate and the true negative rate, where the true-positive and true-negative voxels are computed by applying a threshold on the predicted risk map. The maximum correct classification rate is computed using the optimal threshold which maximizes the correct classification.

Figure 2 shows the prediction results for the slice shown in Figure 1. Shown across the top of Figure 2 are predicted outcomes (by GLM and SAR, respectively) and true outcome. As is evident in the Figure, the GLM yielded a predicted map that is somewhat “speckled” in nature, whereas the SAR model yielded an image that shows greater regional continuity.

The performances of GLM and SAR across all 74 cases are summarized in Table II. Regardless of the metric used, the SAR model provided moderate but statistically significant improvements over GLM in aggregate over all cases. Specifically, using the Student’s *t*-test, the performance of SAR and GLM were found to be different at a statistical significance of $p \leq 0.001$. Individually, GLM outperformed SAR in four cases (5.4%); SAR outperformed GLM in 61 cases (82.4%), and SAR and GLM had comparable performance (i.e., a difference in performance of less than 1%) in 9 cases (12.2%).

5. Discussion and Conclusions

Stroke tissue outcome is an important clinical research problem. Previous methods of tissue outcome prediction have relied upon the use of models which assume voxel-to-voxel independence. In this paper we have utilized the spatial autoregression model to demonstrate that moderate improvements in outcome prediction can be achieved by explicitly incorporating spatial correlations. We have concluded that spatial correlations may be an important factor in analyzing and predicting ischemic stroke outcome, and that spatial autoregressive models may be an effective way of capturing that spatial dependency.

SAR is certainly not the only way of capturing spatial correlations – Markov random field models may be adopted, for example. Spatial correlations can also be incorporated at the data level – for example in the estimation of the perfusion parameters. Lastly, we have in this study neglected the spatial relationship between axial slices due to the poor inter-slice resolution and gap. With suitable 3-D data, spatial correlations may yield greater performance improvement.

One interesting question left open by our study is what is the best achievable performance of stroke prediction, without the use of meta-level knowledge (e.g., (16)). We

obtained moderate performance gains on a dataset of 74 highly heterogeneous samples with respect to age, stroke etiology, imaging time, image acquisition site, etc. We are of the opinion that stroke prediction algorithms can perform to a greater level of accuracy if the sample is large enough to permit patient stratification into more homogeneous groups, and the weighting coefficients are estimated separately on the basis of each group. This heterogeneity may also be part of the reason why SAR worked better in most but not all cases.

Lastly, as with any data analysis method, it is important to reflect upon the assumptions being made by the model. In the case of SAR, we have focused on the hypothesis that accounting for spatial correlations would improve the performance of GLM. It is worthwhile questioning, however, whether a linear model is inherently the correct model for stroke outcome prediction.

References

- 1) Pasternak RC, Criqui MH, Benjamin EJ, Fowkes FG, Isselbacher EM, McCullough PA, Wolf PA, Zheng ZJ. Atherosclerotic Vascular Disease Conference: Writing Group I: epidemiology. *Circulation* 2004;109(21):2605-2612.
- 2) Molina CA, Saver JL. Extending reperfusion therapy for acute ischemic stroke: emerging pharmacological, mechanical, and imaging strategies. *Stroke* 2005;36(10):2311-2320.
- 3) Mullins ME, Schaefer PW, Sorensen AG, Halpern EF, Ay H, He J, Koroshetz WJ, Gonzalez RG. CT and conventional and diffusion-weighted MR imaging in acute stroke: study in 691 patients at presentation to the emergency department. *Radiology* 2002;224(2):353-360.
- 4) Warach S, Chien D, Li W, Ronthal M, Edelman RR. Fast magnetic resonance diffusion-weighted imaging of acute human stroke. *Neurology* 1992;42(9):1717-1723.
- 5) Gonzalez RG, Schaefer PW, Buonanno FS, Schwamm LH, Budzik RF, Rordorf G, Wang B, Sorensen AG, Koroshetz WJ. Diffusion-weighted MR imaging: diagnostic accuracy in patients imaged within 6 hours of stroke symptom onset. *Radiology* 1999;210(1):155-162.
- 6) Sorensen AG, Wu O, Copen WA, Davis TL, Gonzalez RG, Koroshetz WJ, Reese TG, Rosen BR, Wedeen VJ, Weisskoff RM. Human acute cerebral ischemia: detection of changes in water diffusion anisotropy by using MR imaging. *Radiology* 1999;212(3):785-792.
- 7) Kucharczyk J, Mintorovitch J, Asgari H, Tsuura M, Moseley M. In vivo diffusion-perfusion magnetic resonance imaging of acute cerebral ischemia. *Can J Physiol Pharmacol* 1991;69(11):1719-1725.
- 8) Ostergaard L, Sorensen AG, Kwong KK, Weisskoff RM, Gyldensted C, Rosen BR. High resolution measurement of cerebral blood flow using intravascular tracer bolus passages. Part II: Experimental comparison and preliminary results. *Magn Reson Med* 1996;36(5):726-736.
- 9) Jacobs MA, Mitsias P, Soltanian-Zadeh H, Santhakumar S, Ghanei A, Hammond R, Peck DJ, Chopp M, Patel S. Multiparametric MRI tissue characterization in clinical stroke with correlation to clinical outcome: part 2. *Stroke*

2001;32(4):950-957.

- 10) Welch KM, Windham J, Knight RA, Nagesh V, Hugg JW, Jacobs M, Peck D, Booker P, Dereski MO, Levine SR. A model to predict the histopathology of human stroke using diffusion and T2-weighted magnetic resonance imaging. *Stroke* 1995;26(11):1983-1989.
- 11) Wu O, Sumii T, Asahi M, Sasamata M, Ostergaard L, Rosen BR, Lo EH, Dijkhuizen RM. Infarct prediction and treatment assessment with MRI-based algorithms in experimental stroke models. *J Cereb Blood Flow Metab* 2006.
- 12) Wu O, Koroshetz WJ, Ostergaard L, Buonanno FS, Copen WA, Gonzalez RG, Rordorf G, Rosen BR, Schwamm LH, Weisskoff RM, Sorensen AG. Predicting tissue outcome in acute human cerebral ischemia using combined diffusion- and perfusion-weighted MR imaging. *Stroke* 2001;32(4):933-942.
- 13) LeSage JP. Bayesian estimation of limited dependent variable spatial autoregressive models. *Geographical Analysis* 2000;32:19-35.
- 14) LeSage JP, Pace RK. Models for spatially dependent missing data. *J Real Estate Finance and Economics* 2004;29(2):233-254.
- 15) Menezes NM, Ay H, Lopez CJ, Zhu MW, Koroshetz WJ, Aronen HJ, Karonen JO, Nuutinen J, Liu Y, Sorensen AG. "A novel strategy for predicting tissue outcome in acute human stroke". 2005; Miami, FL.
- 16) Menezes NM, Ay H, Wang Zhu M, Lopez CJ, Singhal AB, Karonen JO, Aronen HJ, Liu Y, Nuutinen J, Koroshetz WJ, Sorensen AG. The Real Estate Factor. Quantifying the Impact of Infarct Location on Stroke Severity. *Stroke* 2006.

Table II. Prediction results from 74-patient group.

	GLM	SAR
<i>AUC (area under the ROC curve)</i>	75%	79%
<i>Max correct classification</i>	81%	83%

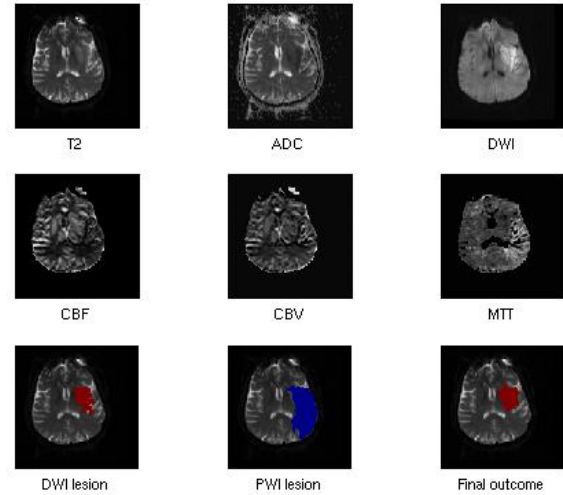


Figure 1. Inputs into the classifier: T2, ADC (apparent diffusion coefficient), DWI (diffusion weighted imaging), CBF (cerebral blood flow), CBV (cerebral blood volume), MTT (mean transit time) images. The DWI lesion, PWI lesion, and Final outcome region, are manually delineated and used by the classifier.

Table I. Distribution of Patients

Category	Number
<i>Total number of studies</i>	74
Male subjects	46
Female subjects	28
Age < 40	4
40 ≤ Age < 50	5
50 ≤ Age < 60	8
60 ≤ Age < 70	15
70 ≤ Age < 80	32
Age ≥ 80	10
<i>Stroke subtype</i>	
Large artery atherosclerosis	21
Cardioembolism	31
Undetermined etiology	16
Other etiology	6
<i>Time of MRI after stroke onset</i>	
T < 3 h	8
3 h ≤ T < 6 h	27
6 h ≤ T < 9 h	29
9 h ≤ T ≤ 12 h	10

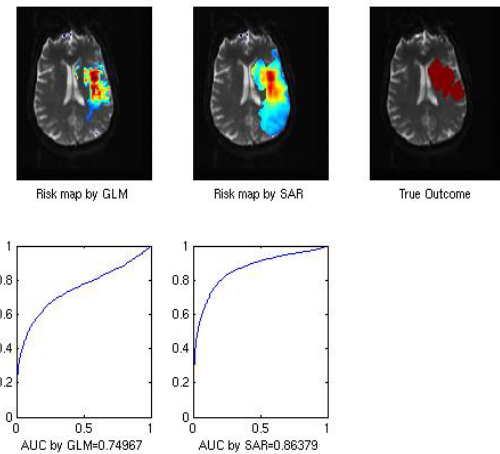


Figure 2. Prediction example of the GLM model and the SAR model. Shown are the risk maps (color overlays thresholded at p=0.3) as predicted by GLM and SAR, for a single patient, along with their respective ROC curves. The final outcome image is also shown.